Inorg. Chem. **2007**, *46*, 10741–10748

Facile Synthesis of BiCuOS by Hydrothermal Methods

William C. Sheets,[†] Evan S. Stampler,[†] Houria Kabbour,[‡] Mariana I. Bertoni,[§] Laurent Cario,[‡] Thomas O. Mason,[§] Tobin J. Marks,[†,§] and Kenneth R. Poeppelmeier*[,†]

Department of Chemistry, Northwestern University, Evanston, Illinois 60208, Institut des Matériaux Jean Rouxel, CNRS-Université de Nantes, 2 rue de la Houssinière, 44322 Nantes Cedex 1, France, and Department of Materials Science and Engineering, Northwestern University, Evanston, Illinois 60208

Received July 23, 2007

BiCuOS, which is isostructural to the layered rare-earth oxysulfides LnCuOS (Ln = La–Eu), was synthesized by a single-step hydrothermal reaction at low temperature (250 °C) and pressure (<20 atm). Particular emphasis is placed on how the selection of the proper reaction conditions, such as temperature and pH, achieves a mutual high solubility of the metal–oxide reactants, Bi_2O_3 and Cu_2O, and thus generates BiCuOS in a good yield. The optical and electrical properties of BiCuOS were measured to determine the influence of replacing a rare-earth cation with bismuth. The electrical conductivity of BiCuOS is increased over that of certain layered rare-earth oxysulfides, LnCuOS (Ln = La, Pr, and Nd), and is similar to that of the cerium members, CeCuOS and CeAgOS. Band structure calculations reveal that, similar to other potential transparent conductors containing sixth-row elements, relativistic effects significantly lower the energy of the conduction band, and thus narrow the optical band gap. These low-energy conduction bands are responsible for the electrical and optical properties of BiCuOS.

Introduction

Since Ueda and co-workers reported that LaCuOS has an optical band gap of 3.1 eV and exhibits *p*-type electrical conductivity,[1] the quaternary rare-earth copper oxychalcogenides, especially the sulfide members, have received considerable attention, owing to their potential application as *p*-type transparent conductors. Figure 1 shows the LaCuOS crystal structure, which belongs to the ZrSiCuAs structure type in the tetragonal *P*4/*nmm* space group.[2,3] The composite crystal structure is composed of anti-fluorite-like $(Cu_2S_2)^{2-}$ layers, which consist of edge-sharing CuS_4 tetrahedra, alternately stacked with fluorite-like $(La_2O_2)^{2+}$ layers along the *c* axis of the tetragonal cell. The layered structure with the oxide and sulfide layers clearly separated (i.e., the Cu^+ cations are coordinated exclusively by S^{2-} anions) is responsible for the unique electrical and optical properties of LaCuOS.[4] In this structure, the covalent $(Cu_2S_2)^{2-}$ layers form the conduction pathway for hole transport; however, the ionic $(La_2O_2)^{2+}$ layers confine the Cu−S bonds to the 2D $(Cu_2S_2)^{2-}$ layers, thereby preserving the transparency of LaCuOS.[5] Moreover, the presence of a more-electropositive

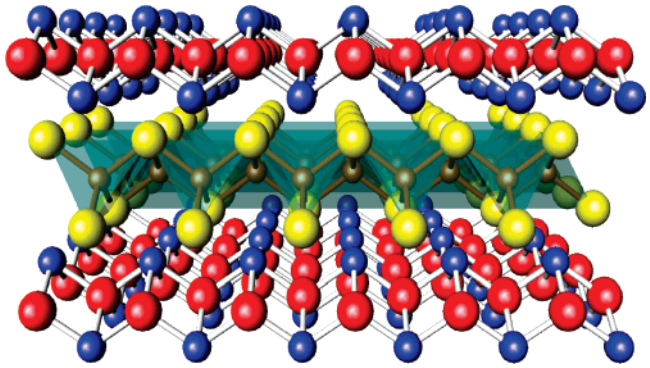

Figure 1. Schematic representation of the LaCuOS structure along the (100) axis, which is composed of $(La_2O_2)^{2+}$ and $(Cu_2S_2)^{2-}$ layers. For clarity, no La−S bonds are shown. Blue, brown, red, and yellow spheres represent La^{3+}, Cu^+, O^{2-}, and S^{2-} ions, respectively. Green polyhedra are used to define the edge-sharing CuS_4 tetrahedra.

* To whom correspondence should be addressed. Email: krp@northwestern.edu.
† Department of Chemistry, Northwestern University.
‡ CNRS-Université de Nantes.
§ Department of Materials Science and Engineering, Northwestern University.

(1) Ueda, K.; Inoue, S.; Hirose, S.; Kawazoe, H.; Hosono, H. *Appl. Phys. Lett.* **2000**, *77* (17), 2701−2703.
(2) Palazzi, M. *C. R. Acad. Sci.* **1981**, *292* (10), 789−791.
(3) Johnson, V.; Jeitschko, W. *J. Solid State Chem.* **1974**, *11*, 161−166.
(4) Inoue, S.-i.; Ueda, K.; Hosono, H.; Hamada, N. *Phys. Rev. B: Condens. Matter* **2001**, *64* (24), 245211/1−245211/5.
(5) Ueda, K.; Inoue, S.; Hosono, H.; Sarukura, N.; Hirano, M. *Appl. Phys. Lett.* **2001**, *78* (16), 2333−2335.

10.1021/ic7014622 CCC: $37.00
Published on Web 11/14/2007

rare-earth ion (e.g., La^{3+}) in the structure is important because its inductive effect shifts the conduction band toward higher energy and thus increases the optical band gap.

The oxychalcogenide members of the ZrSiCuAs structure-type can accommodate a wide variety of trivalent cations (La−Ho, Y, and Bi), monovalent group-13 cations (Cu and Ag) and chalcogenides (S, Se, and Te), and such materials have been studied for the various properties afforded by this compositional versatility.[6−9] Specifically, the optical and electrical transport properties of the quaternary rare-earth copper oxychalcogenides have been previously altered by elemental substitution on both the rare earth and chalcogenide sites. For example, systematically increasing the selenium content in $LaCuOS_xSe_{1-x}$ incrementally increases the Hall mobility and conductivity but decreases the optical band gap.[10] When optimized, magnesium-doped LaCuOSe thin films exhibit a *p*-type degenerate semiconducting behavior with a respectable room-temperature conductivity of 140 S cm^{-1}. Moreover, to examine the influence of the rare-earth ions on the optical and electrical transport properties, another study focused on the replacement of the La^{3+} ions in LaCuOS with several other rare-earths (Ce^{3+}, Pr^{3+} and Nd^{3+}), which were chosen on the basis of similar ionic radii.[11] The optical and electrical properties of both nondoped and strontium-doped PrCuOS and NdCuOS were comparable to those of nondoped and strontium-doped LaCuOS, respectively. However, nondoped CeCuOS is black and exhibits electrical conductivity that is nearly as high as that of the doped rare-earth materials (0.61 S cm^{-1}). The authors proposed a shift in the conduction band states of CeCuOS to form an unoccupied band near the Fermi level, which accounts for the color and semimetallic characteristics.[11] A similar conductivity of 0.16(4) S cm^{-1} has been reported for isostructural CeAgOS.[8] All things considered, the various cation and anion substitutions provide some measure of modifying the optical and electrical properties of quaternary rare-earth copper oxychalcogenides.

The synthesis of oxychalcogenides in aqueous solution is challenging because there is a thermodynamic preference for the formation of the oxide and/or complex oxoanion (e.g., SO_4^{2-}, $S_2O_3^{2-}$, and SO_3^{2-}). The majority of oxychalcogenides synthesized by hydrothermal methods belong to the family of cetineite-type compounds, $A_6[Sb_{12}O_{18}][SbX_3]_2 \cdot x[H_2O]$ where A = Na^+, K^+, Rb^+ and X = S^{2-}, Se^{2-}, and Te^{2-}, which have been studied extensively owing to their potential application as semiconducting nanoporous crystalline solids.[12−15] These cetineite-type phases result from the hydrothermal reaction of elementary antimony and chalcogenide in an aqueous NaOH or KOH solution. Another example of a hydrothermally synthesized oxychalcogenide is Bi_2O_2S, which was prepared in a reaction between a 2:1 stoichiometric mixture of Bi_2O_3 and Bi_2S_3 in a 10% NaOH solution heated to 400 °C under 98 MPa pressure for 3 days.[16] Higher pressures and temperatures are required in this reaction to overcome the low solubility of metal sulfides in aqueous solutions. Subsequent syntheses of isostructural-doped Y_2O_2S and La_2O_2S phosphors have utilized solvothermal methods.[17]

Samples of BiCuOS have been synthesized previously by a high-temperature reaction in evacuated sealed quartz ampoules.[18] However, the optical and electrical properties of BiCuOS have not been studied in depth. Avoiding the long annealing times required for the quartz ampule syntheses, we report here the low-temperature hydrothermal synthesis of BiCuOS. Owing to the challenge in synthesizing oxychalcogenides by hydrothermal methods, we detail how the more-acidic character of amphoteric Bi_2O_3, compared to the very basic character of the rare-earth sesquioxides, enhances its solubility under mild hydrothermal conditions and thus explains why BiCuOS forms and LnCuOS compounds do not. The optical and electrical properties of BiCuOS also are presented and compared with those of LnMOS (Ln = La−Nd and M = Cu, Ag) and other metal oxides containing bismuth, thereby permitting discussion of the influence of bismuth on the properties.

Experimental Section

Synthesis. Samples of polycrystalline BiCuOS were prepared from the direct hydrothermal reaction between Bi_2O_3 (99.99%, Alfa Aesar), Cu_2O (99.9%, Alfa Aesar), and Na_2S. Before use, $Na_2S \cdot 9H_2O$ (98+%, Aldrich) is heated in a vacuum oven for 24 h at approximately 125 °C to remove a large fraction of the water, thereby fusing the material. Stoichiometric amounts (0.92 mmol of Bi_2O_3 and Cu_2O, 1.84 mmol of Na_2S; 1.0 g total mass) of these reagents were charged into a 125 mL poly(tetrafluoroethylene) (PTFE) Teflon-lined pressure vessel (Parr Instruments), which was then backfilled with 75 mL of distilled water. The pressure vessel was then sealed and heated to 150 °C, followed by a controlled incremental temperature increase over 5 h to 250 °C. The maximum temperature was then held constant for 48 h, with subsequent cooling to room temperature. After the latter step, the polycrystalline BiCuOS products were recovered by filtration, followed by a deionized water rinse. The mass yield of the reaction is >80% (calculated on bismuth).

(6) Charkin, D. O.; Akopyan, A. V.; Dolgikh, V. A. *Zh. Neorg. Khim.* **1999**, *44* (6), 895−899.
(7) Ueda, K.; Hiramatsu, H.; Hirano, M.; Kamiya, T.; Hosono, H. *Thin Solid Films* **2006**, *496* (1), 8−15.
(8) Chan, G. H.; Deng, B.; Bertoni, M.; Ireland, J. R.; Hersam, M. C.; Mason, T. O.; Van Duyne, R. P.; Ibers, J. A. *Inorg. Chem.* **2006**, *45* (20), 8264−8272.
(9) Liu, M. L.; Wu, L. B.; Huang, F. Q.; Chen, L. D.; Ibers, J. A. *J. Solid State Chem.* **2007**, *180* (1), 62−69.
(10) Ueda, K.; Hosono, H. *J. Appl. Phys.* **2002**, *91* (7), 4768−4770.
(11) Ueda, K.; Takafuji, K.; Hiramatsu, H.; Ohta, H.; Kamiya, T.; Hirano, M.; Hosono, H. *Chem. Mater.* **2003**, *15* (19), 3692−3695.
(12) Simon, U.; Schuth, F.; Schunk, S.; Wang, X. Q.; Liebau, F. *Angew. Chem., Int. Ed.* **1997**, *36* (10), 1121−1124.
(13) Starrost, F.; Krasovskii, E. E.; Schattke, W.; Jockel, J.; Simon, U.; Wang, X.; Liebau, F. *Phys. Rev. Lett.* **1998**, *80* (15), 3316−3319.
(14) Wang, X.; Liebau, F. *Z. Kristallogr.* **1999**, *214* (12), 820−834.
(15) Shulman, A.; Palmqvist, A. E. C. Recent developments in the synthesis of the microporous semiconductor SBC-1. In *Recent Advances in the Science and Technology of Zeolites and Related Materials, Pts A - C*; 2004; Vol. 154, pp 1137−1144.
(16) Koyama, E.; Nakai, I.; Nagashima, K. *Acta Crystallogr., Sect. B* **1984**, *40* (APR), 105−109.
(17) Kuang, J. Y.; Liu, Y. L.; Yuan, D. S. *Electrochem. Solid State Lett.* **2005**, *8* (9), H72−H74.
(18) Kusainova, A. M.; Berdonosov, P. S.; Akselrud, L. G.; Kholodkovskaya, L. N.; Dolgikh, V. A.; Popovkin, B. A. *J. Solid State Chem.* **1994**, *112* (1), 189−191.

Powder X-ray Analysis. Powder X-ray diffraction (PXD) data were recorded on a Scintag XDS 2000 diffractometer operating at 40 kV and 20 mA with nickel-filtered Cu Kα radiation. Data were collected in the 10 to 80° 2θ range by pausing in 0.05° steps for 1 s. The PXD pattern of BiCuOS was matched to the JCPDS file 47−227 using the *Jade* software suite,[19] and the unit cell parameters were refined by the Rietveld method in GSAS. Moreover, the experimental powder data were matched to a calculated PXD pattern generated from published crystallographic data by the *PowderCell* software suite.[20]

Electron Microscopic Analysis. Electron microscopy studies of BiCuOS were carried out using a Hitachi S-4500 scanning electron microscope (SEM). To prepare SEM samples, polycrystalline samples were attached to an aluminum mount using carbon tape and then coated with 5 nm of gold. Energy-dispersive X-ray (EDX) analysis (Hitachi S-3500 SEM) was used to analyze the stoichiometry of the sample. Analysis confirmed the samples to have a stoichiometric ratio of bismuth, copper, and sulfur, within the limit of accuracy of the EDX technique; oxygen was observed but not quantified (EDX spectrum in the Supporting Information).

Optical Analysis. Optical data were obtained via diffuse reflectance. In a diffuse reflectance experiment, the nonspecular component of reflection (i.e., radiation that has undergone multiple scattering events on different particles and returned to the sample surface) is measured relative to a standard.[21] Diffuse reflectance data were collected over the spectral range 200−800 nm using a Cary 500 scanning double beam spectrophotometer equipped with an integrating sphere (110 mm in diameter; Cary 1E with Cary 1/3 attachment, Varian Walnut Creek, CA). Baseline spectra were collected on pressed PTFE Halon placed in the sample and reference beams. Data were collected with a scan rate of 150 nm min^{-1}, a data interval of 0.5 nm, an average step time of 0.2 s, and a signal bandwidth of 3 nm. Pellets were mounted on a blackened sample mask. The reflectance data were translated into absorption data (α/S) using an equation developed by Kubelka and Munk, $\alpha/S = (1 - R)^2/2R$, where α is the absorption coefficient, S is the scattering coefficient, and R is the diffuse reflectance at a certain energy.[22]

Conductivity Measurements. The electrical conductivity of the as-prepared polycrystalline BiCuOS was obtained by the powder-solution-composite (PSC) technique.[23] In this technique, the bulk conductivity of a ceramic powder is obtained by measuring the impedance spectra of the composite slurries of the powder with electrolytic solutions of NaCl. Powder conductivity is obtained from a series of experiments in which the conductivity of the aqueous electrolytic solution phase is varied from 2.6×10^{-4} (0.002 M) to 0.25 S cm^{-1} (4.8 M). Each of these solutions was mixed with 0.09 g of BiCuOS powder to form a slurry, which was then placed in the measuring apparatus (described elsewhere in detail)[23] and allowed to settle. The application of this technique to materials with known conductivities produces results that are in good agreement with expected values.

Electronic Structure Calculations. Linear muffin-tin orbital (LMTO) calculations[24,25] on BiCuOS were performed within the atomic sphere approximation using version 47C of the *Stuttgart TB-LMTO-ASA* program.[26] Scalar-relativistic Kohn−Sham equations within the local density approximation[27] were solved taking all of the relativistic effects into account except for the spin−orbit coupling. The calculations were performed on 484 irreducible k points within the primitive wedge of the Brillouin zone. Calculations were performed on the ideal crystal structure of BiCuOS (space group *P4/nmm*, $a = 3.8705$ Å, $c = 8.561$ Å)[18] displayed in Figure 1. LMTO calculations were also performed on the *P4/nmm* crystal structure of LaCuOS, taken from the structural report by Ueda et al.[10] A grid of 484 irreducible k points that were within the primitive edge of the Brillouin zone was used for the calculation on LaCuOS.

Results and Discussion

As summarized by Rabenau, for preparative hydrothermal reactions a solubility of 2−5% for the least-soluble component is a necessary condition to generate the product in high yield.[28] Whereas Na_2S dissolves readily, at room temperature the metal−oxide reactants Bi_2O_3 and Cu_2O are insoluble; however, an increase in temperature and/or the use of a mineralizer provides an effective mechanism to increase their solubility. Thus, reaction conditions, primarily temperature and pH, were chosen in which Bi_2O_3 and Cu_2O dissolve, and their corresponding cation complexes are readily soluble. Although alkali hydroxides are effective mineralizers for metal oxides,[29] they were not used to avoid hydrolysis of the sulfide, itself a weak base.[28] Acidic mineralizers such as HNO_3, HCl, and H_2SO_4 also could not be used because of their propensity to either incorporate their corresponding anions into the reaction product or react immediately with the starting materials to form chemically inert precipitates. Specifically, these acids promoted Cu_2O disproportionation to copper metal and aqueous Cu^{2+} species, the latter stabilized as the corresponding nitrates, chlorides, and sulfates.[30] For the same reason, metal nitrates and halides, which are common hydrothermal precursors, were avoided. As a result, an increase in the reaction temperature was necessary to dissolve the metal−oxide reactants. Indeed, the solubility of α-Bi_2O_3 (bismite), measured by UV spectrophotometry, has been reported to increase with temperature to a maximum of 10^{-3} mol L^{-1} for a neutral solution at 250 °C,[31,32] a marked 100-fold increase over the reported room temperature solubility of 10^{-5} mol L^{-1} for α-Bi_2O_3 at neutral pH.[33] Such solubility would represent 10% of the reactant Bi_2O_3 in solution for the described reaction conditions. Both the room and elevated temperature studies report soluble $Bi(OH)_3$ and $Bi(OH)_4^-$ species to be the principal hydrolysis products in slightly basic aqueous solutions. Similarly, the

(19) *Jade*, version 5.0; Materials Data Inc.: Livermore, CA, 1999.
(20) *PowderCell*, version 2.4; Federal Institute for Materials Research and Testing: Berlin, Germany, 2000.
(21) Hecht, H. G. *Mod. Aspects Reflectance Spectrosc. Proc. Symp. Chicago* **1968**, 1−26.
(22) Kubelka, P.; Munk, F. *Z. Tech. Phys. (Leipzig)* **1931**, *12*, 593.
(23) Ingram, B. J.; Mason, T. O. *J. Electrochem. Soc.* **2003**, *150* (8), E396−E402.
(24) Andersen, O. K. *Phys. Rev. B: Solid State* **1975**, *12* (8), 3060−3083.
(25) Jepsen, O.; Andersen, O. K. *Z. Phys. B Condens. Matter* **1995**, *97* (1), 35−47.
(26) Jepsen, O.; Andersen, O. K. *The Stuttgart TB-LMTO-ASA Program*, version 47; MPI fur Festkorperforschung: Stuttgart, Germany, 2000.
(27) Von Barth, U.; Hedin, L. *J. Phys. C: Solid State Phys.* **1972**, *5* (13), 1629−1642.
(28) Rabenau, A. *Angew. Chem., Int. Ed.* **1985**, *24*, 1026−1040 and references therein.
(29) Sheets, W. C.; Mugnier, E.; Barnabe, A.; Marks, T. J.; Poeppelmeier, K. R. *Chem. Mater.* **2006**, *18* (1), 7−20.
(30) Kamau, P.; Jordan, R. B. *Inorg. Chem.* **2001**, *40* (16), 3879−3883.
(31) Kolonin, G. R.; Laptev, Y. V. *Geokhimiya* **1982**, *11*, 1621−31.
(32) Laptev, Y. V.; Kolonin, G. R. *Zh. Neorg. Khim.* **1982**, *27* (10), 2515−20.
(33) Baes, C. F., Jr.; Mesmer, R. E. *The Hydrolysis of Cations*; Krieger Publishing Company: Malabar, FL, 1976.

dissolution of Cu_2O and stabilization of Cu^+ represent important components of the present reactions. In aqueous solution at room temperature and ambient pressure, it is well-known that Cu^+ ions disproportionate to Cu^{2+} ions and copper metal.[34,35] At elevated temperatures, however, the stability of the aqueous Cu^+ species increases because the decreased water dielectric constant destabilizes the more highly charged Cu^{2+} ion, thereby reducing the driving force for disproportionation. An important feature of the present synthesis, therefore, is the implementation of hydrothermal water as a reaction medium. At elevated temperatures and basic pH, Cu_2O dissolves to form stable, soluble Cu(OH) and $Cu(OH)_2^-$ species.[36,37] Cu^+ species, although stable, are limited in their solubility in alkaline aqueous media, with an estimated maximum reported to be 10^{-4} mol L^{-1} at 200 °C.[38,39] The solubility data summarized above for copper are from the Pourbaix (potential pH) diagram describing the simple $Cu-H_2O$ system, however, and do not consider the presence of sulfides in the solution. In fact, the data reported in Pourbaix diagrams for the $Cu-S-H_2O$ system indicate that interactions between Cu^+ and the various sulfides species occur, and that the copper thio-complex $Cu(HS)_2^-$ predominates in basic aqueous solutions.[40] The aqueous HS^- species results from the hydrolysis of S^{2-} at elevated temperatures because S^{2-} is a sufficiently strong base to undergo hydrolysis below pH 14. Nevertheless, there is a limited region of overlap between the stability domains of the copper hydroxide and sulfide complexes.[41] Without knowledge of the complexation kinetics for both OH^- and HS^- with Cu^+, and because an accurate in situ measurement of the reduction potential does not exist, the dominant aqueous form of Cu^+ cannot be established with certainty. Nevertheless, Cu_2O dissolves and remains soluble under the reaction conditions to allow BiCuOS to form in high yield.

Upon optimization of the reaction temperature and mineralizer concentration, BiCuOS is formed in the direct reaction between Bi_2O_3, Cu_2O, and Na_2S. This reaction produces BiCuOS on a gram scale in 48 h, significantly less time than the 600 h (25 d) required for the solid-state reaction. Similar attempts to synthesize other LnCuOS (Ln = La − Lu) phases resulted in the formation of either $Ln(OH)_3$ (Ln = La − Ho) or LnOOH (Ln = Er − Lu) in addition to a variety of copper sulfides, such as anilite ($Cu_{1.75}S$) and digenite ($Cu_{1.8}S$), among others.

As illustrated by the SEM images in Figure 2, crystallite sizes for the as-prepared BiCuOS samples range from a few tenths of a micrometer to ∼2 μm. Figure 3 shows a representative powder X-ray diffraction (PXD) pattern of a

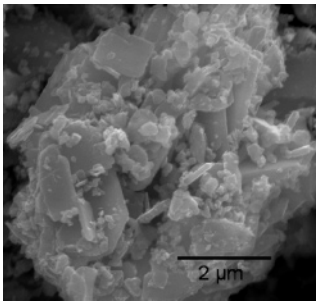

Figure 2. SEM image of an agglomerate of BiCuOS crystallites ranging in size from a few tenths of a micrometer up to ∼2 μm.

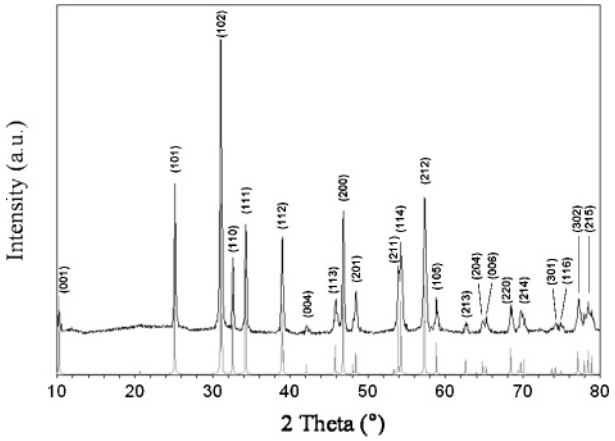

Figure 3. PXD pattern of the BiCuOS product. Calculated positions, both indexed and indicating relative intensities, are shown in gray.

phase-pure sample, which can be indexed as BiCuOS (JCPDS 47−0277, $a = 3.868$ Å, $c = 8.561$ Å, space group *P4*/*nmm*) with a tetragonal unit cell. The refined unit cell parameters for BiCuOS, $a = 3.8708(8)$ Å, $c = 8.558(1)$ Å are in good agreement with those reported previously for a single-crystal sample, $a = 3.8705(5)$, $c = 8.561(1)$ Å.[18] Whereas a majority of the reactions generate phase-pure BiCuOS, some reactions yielded products that contained unreacted Bi_2O_3 and/or trace amounts of the alternate phases $Cu_{1.8}S$ and Cu_3BiS_3. Lower reaction temperatures (<240 °C) increase the yield of Bi_2O_3, $Cu_{1.8}S$, and Cu_3BiS_3. Indeed, Cu_3BiS_3 has been synthesized previously by a low-temperature (100−150 °C) hydrothermal decomposition process, incorporating CuCl and $BiCl_3$ in a water/NH_2CSNH_2 solvent mixture.[42] Samples where only BiCuOS and Bi_2O_3 are present were treated with dilute HCl (1:1) to remove any unreacted Bi_2O_3. This treatment does not appear to decompose BiCuOS, a conclusion that was confirmed by PXD. No acid or solvent, however, could be found that preferentially removes the Cu_3BiS_3 and $Cu_{1.8}S$ phases versus the BiCuOS phase.

As mentioned previously, whereas BiCuOS can be synthesized readily under the present conditions, hydrothermal syntheses of LnCuOS phases (Ln = La−Nd, Sm−Lu) from Ln_2O_3, Cu_2O, and Na_2S were unsuccessful. In these reactions, $Ln(OH)_3$ was the primary product for the early rare-earths (La−Ho) under similar reaction conditions ($T = 250$ °C, pH

(34) Latimer, W. M. *The Oxidation States of the Elements and Their Potentials in Aqueous Solutions.* 2nd ed.; Prentice Hall: New York, 1964.
(35) Kolthoff, I. M.; Coetzee, J. F. *J. Am. Chem. Soc.* **1957**, *79*, 1852−8.
(36) Var'yash, L. N.; Rekharskii, V. I. *Geokhimiya* **1981**, *5*, 683−8.
(37) Beverskog, B.; Puigdomenech, I. *J. Electrochem. Soc.* **1997**, *144* (10), 3476−3483.
(38) Var'yash, L. N. *Geokhimiya* **1989**, *3*, 412−22.
(39) Var'yash, L. N. *Geokhimiya* **1991**, *8*, 1066−74.
(40) Young, C. A.; Dahlgren, E. J.; Robins, R. G. *Hydrometallurgy* **2003**, *68* (1−3), 23−31.
(41) Protopopoff, E.; Marcus, P. *Corros. Sci.* **2003**, *45* (6), 1191−1201.
(42) Hu, J.; Deng, B.; Wang, C.; Tang, K.; Qian, Y. *Mater. Chem. Phys.* **2003**, *78* (3), 650−654.

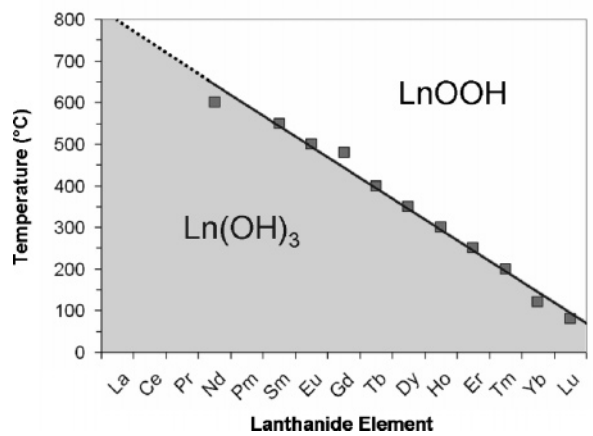

Figure 4. Graph illustrating the temperature boundary (the line is drawn as a guide to the eye) that separates the stability ranges of rare-earth trihydroxides from the rare-earth oxide hydroxides in hydrothermal conditions. Adapted from Klevtsov.[45]

7). This is not surprising given the basicity of the rare-earth oxides, and therefore their solubility in nonacidic aqueous solutions is negligible at room temperature.[43] In fact it is well-known that rare-earth sesquioxides readily undergo hydrolysis to generate the stable, insoluble trihydroxide in water at room temperature. Whereas, in general, an increase in temperature can favor the less-hydrated solid oxide phase, the rare-earth trihydroxides are stable and persist at elevated temperatures. For example, $La(OH)_3$ is stable up to 800 °C under hydrothermal conditions.[44] However, the basicities of the rare-earth trihydroxides decrease with increasing atomic number, as would be expected from the decrease in the ionic radius.[45] As shown in Figure 4, the late rare-earth trihydroxides (Er−Lu) transitions to the more-reactive rare-earth oxide hydroxide at lower temperatures (<250 °C), reaction conditions that are compatible with Teflon-lined pressure vessels. Nevertheless, attempts to synthesize LnCuOS phases (Ln = Er − Lu) were also unsuccessful, and LnOOH was the primary reaction product. The smaller cation radius of the late rare-earths, and not their solubility, prevents the formation of LnCuOS (Ln = Er − Lu). According to a study by Popovkin et al., cations smaller than Eu^{3+} (r^{3+}_{VIII} < 1.066 Å)[46] cause the $(Ln_2O_2)^{2+}$ layer to be geometrically incommensurate with the $(Cu_2S_2)^{2-}$ layer.[47] In fact, smaller rare-earth cations deform the CuS_4 tetrahedra past their limit of distortion because the Cu−Cu separation becomes too small.

The synthetic route used here differs from those used previously. LaCuOS was prepared initially by Palazzi through the oxidation of $LaCuS_2$.[2] Since then, solid-state reactions of binary starting materials (e.g., La_2S_3, Cu_2S, and La_2O_3) in evacuated silica tubes/ampules have been used commonly to prepare both single-crystal and polycrystalline-layered oxychalcogenide samples.[1,8] The sealed silica-tube

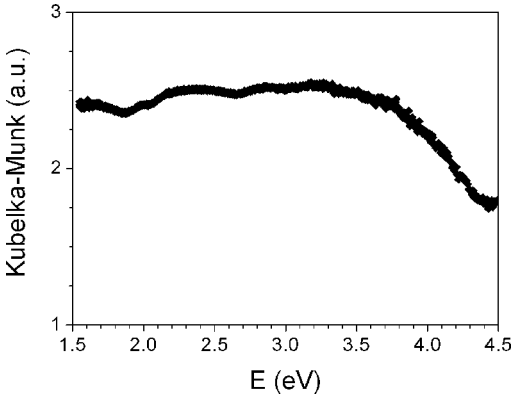

Figure 5. Kubelka−Munk absorption spectra of as-prepared BiCuOS with respect to a PTFE Halon standard.

synthetic method was later extended to generate the heavier rare-earth and telluride members of the copper oxychalcogenides.[9,6] Certain layered rare-earth and bismuth copper oxychalcogenides, having the general formula MCuOQ, where M = Nd, Gd, Dy, Bi, and Q = S, Se, require a reaction between the rare-earth or bismuth oxide combined with elemental chalcogenide and copper metal.[18] These syntheses proved time-consuming, however, as annealing for 300 h at 720 °C in evacuated sealed quartz ampules is necessary to form phase-pure specimens. In the case of BiCuOS, the annealing time is 600 h (25 days).

The optical properties of BiCuOS were studied with diffuse reflectance. Spectra collected on a uniaxially cold-pressed, polycrystalline specimen (150 MPa) are shown in Figure 5. The absorption of BiCuOS is high across the entire visible region (2−3 eV), not surprising given the black color of the sample. This indicates that the optical band gap of BiCuOS is much smaller (<1.5 eV) than that of the isostructural rare-earth copper chalcogenides (e.g., 3.1 eV for LaCuOS).[7,48] Indeed, the LMTO-calculated band structure (Figures 6) and projected density of the states (Figure 7) indicate that the small BiCuOS band gap is a result of low-energy bismuth 6*p*, sulfur 3*p*, and oxygen 2*p* states that are close in energy to the top of the valence band. The conduction band minimum (CBM) of BiCuOS is located at the Γ point, whereas the valence band maximum (VBM) is located between the Γ and M points, and the indirect band gap between these points is nearly zero. Similar to isostructural CeAgOS, the transitions from different symmetries may be weak or forbidden.[8] A direct band gap of 0.5 eV can be assigned to the Z point, which is also similar to the 0.71 eV value measured for CeAgOS. In BiCuOS, the bismuth 6*p* states are mainly empty, as expected for a formally Bi^{3+} system, and form the conduction band (part a of Figure 6). The low energy of these bismuth 6*p* states can be attributed to scalar relativistic effects associated with sixth-row elements.[49] The relativistic effects lower the energy of the bismuth 6*p* orbitals, thereby lowering the energy of the conduction band and decreasing the band gap. In contrast,

(43) Deberdt, S.; Castet, S.; Dandurand, J.-L.; Harrichoury, J.-C.; Louiset, I. *Chem. Geol.* **1998**, *151* (1−4), 349−372.
(44) Viswanathiah, M. N.; Tareen, J. A. K.; Kutty, T. R. N. *Mater. Res. Bull.* **1980**, *15* (7), 855−9.
(45) Klevtsov, P. V.; Sheina, L. P. *Izv. Akad. Nauk, Neorg. Mater.* **1965**, *1* (6), 912−17.
(46) Shannon, R. D. *Acta Crystallogr. Sect. A* **1976**, *A32* (5), 751−67.
(47) Popovkin, B. A.; Kusainova, A. M.; Dolgikh, V. A.; Aksel'rud, L. G. *Zh. Neorg. Khim.* **1998**, *43* (10), 1589−1593.
(48) Ueda, K.; Hosono, H.; Hamada, N. *J. Phys. Condens. Matter* **2004**, *16* (28), 5179−5186.
(49) Pyykko, P. *Chem. Rev.* **1988**, *88* (3), 563−94.

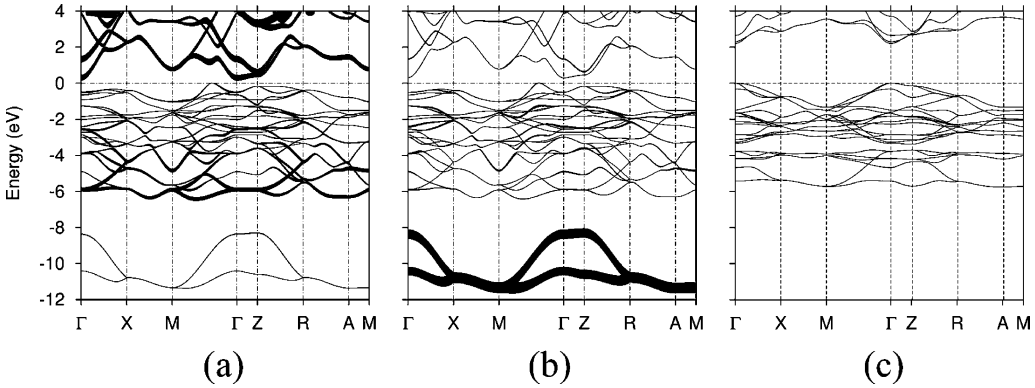

Figure 6. Calculated band structures for (a) BiCuOS *p* states, (b) BiCuOS *s* states, and (c) LaCuOS. The fat bands show the bismuth (a) *p* state contribution and the (b) *s* state contribution to the band structure. In this plot, the top of the valence band is taken as zero on the energy axis.

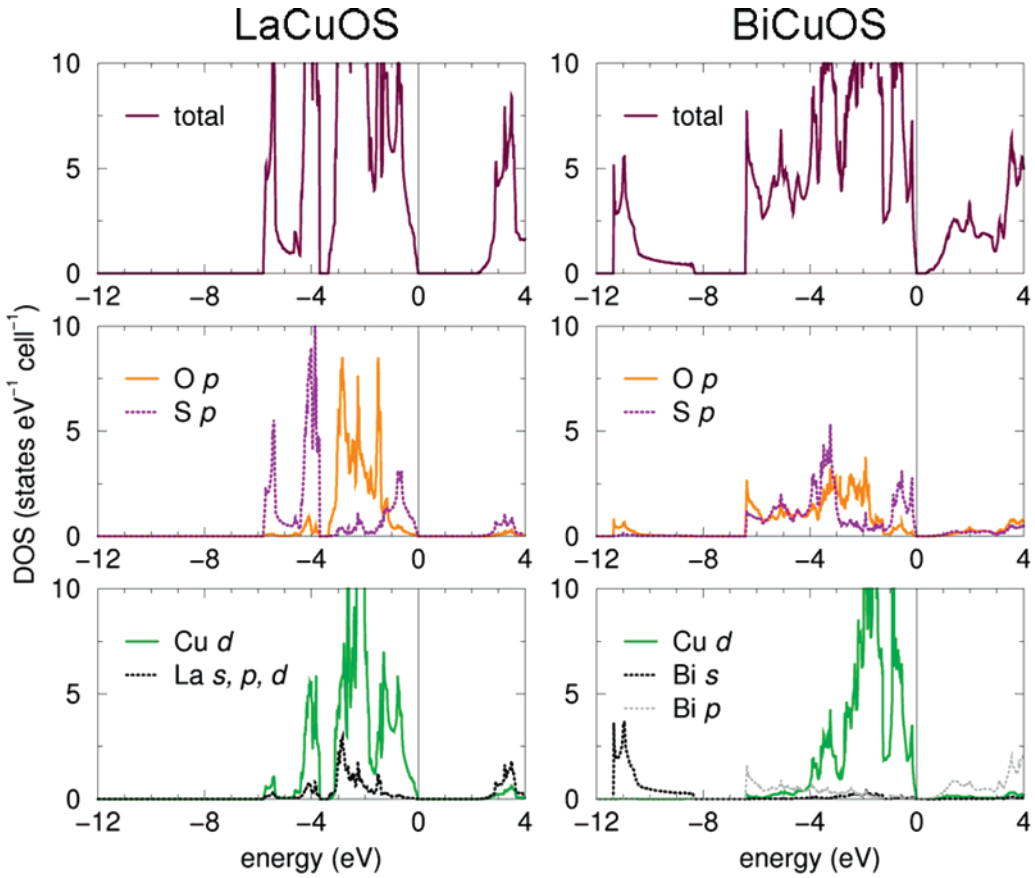

Figure 7. Projected LMTO densities of states (DOS), with each atomic contribution highlighted in color, for LaCuOS (left) and BiCuOS (right). In this plot, the top of the valence band is taken as zero on the energy axis.

as seen in part c of Figure 6, the band gap of LaCuOS is much larger. Although the orbital contribution to the valence bands of LaCuOS is similar to that of BiCuOS (copper 3*d*, sulfur 3*p* states, and oxygen 2*p* states), the CBM of LaCuOS is composed of copper 4*s* and lanthanum 5*d* states at much-higher energy (Figure 7), as evidenced by the high optical transparency of this material in the visible region.[1]

The optical data for BiCuOS can be compared with those obtained from experimental and computational studies on other potential transparent conducting materials containing sixth-row elements, where relativistic effects also decrease the optical band gap. For example, the small optical band gap of $PbCu_2O_2$ (∼1.7 eV) precludes its use as a transparent conductor;[50] however, the structurally similar $SrCu_2O_2$ is a transparent *p*-type conductor with an optical band gap of 3.3 eV.[51] Similarly, a reduction in the optical band gap owing to relativistic effects has been reported in a detailed study of the electronic structure of main-group oxides containing edge-sharing octahedra for application as *n*-type transparent conductors.[52] Through a combination of diffuse reflectance experiments, band structure calculations, and literature data

(50) Yanagi, H.; Tate, J.; Nagarajan, R.; Sleight, A. W. *Solid State Commun.* **2002**, *122* (6), 295−297.
(51) Kudo, A.; Yanagi, H.; Hosono, H.; Kawazoe, H. *Appl. Phys. Lett.* **1998**, *73* (2), 220−222.
(52) Mizoguchi, H.; Woodward, P. M. *Chem. Mater.* **2004**, *16* (25), 5233−5248.

analysis, the authors noted that the optical band gaps of the antimonates $NaSbO_3$ (4.9 eV), $MgSb_2O_6$ (4.3 eV), $SrSb_2O_6$ (5.0 eV), $BaSb_2O_6$ (>5.5 eV), and $ZnSb_2O_6$ (3.5 eV) are considerably larger than those of the analogous bismuthates $NaBiO_3$ (2.7 eV), $MgBi_2O_6$ (1.8 eV), $SrBi_2O_6$ (2.0 eV), $BaBi_2O_6$ (2.6 eV), and $ZnBi_2O_6$ (1.7 eV). With respect to these compounds, LMTO calculations indicated that relativistic effects lower the energies and decrease the spatial extent of the CBM, which comprise the empty bismuth 6*s* orbitals. Both of these trends reduce the overlap between bismuth and oxygen, decreasing the antibonding character of the CBM and thereby substantially lowering its energy.[52] As a result, the band gaps of the bismuthates are decreased significantly. With respect to BiCuOS, parts a and b of Figure 6 illustrate that the conduction band of BiCuOS is composed primarily of bismuth 6*p* states and not bismuth 6*s* states as with the previously discussed bismuthates, formally Bi^{5+} systems. In BiCuOS, the dominant contribution of the filled bismuth 6*s* orbitals is not near the band gap (part b of Figure 6, Figure 7) but is found in a window of energy around −8 to −12 eV with respect to the top of the valence band (set as the origin of the energy axis in this and other plots). The location of the bismuth 6*s* states is similar to that of other bismuth oxides with bismuth in a formal Bi^{3+} oxidation state.[53,54] Overall, these results highlight the challenge in designing transparent conductors based on lead or bismuth oxides owing to the pronounced relativistic effects associated with sixth-row elements.

Because the BiCuOS samples could not be sintered into bulk ceramics without partial or complete thermal decomposition, a powder-solution-composite (PSC) technique[23] was used to characterize their electrical properties. The electrical conductivity of multiple composite slurries composed of BiCuOS powders and electrolyte solutions of varying NaCl concentration was determined with AC-impedance spectroscopy. Mixing-law and effective-media theories are then used to describe the electrical behavior of the composite NaCl/BiCuOS slurry, depending upon particle morphology and size distribution.[55−59] SEM images (Figure 2) indicate a similar platelike particle morphology for all of the BiCuOS samples, and thus the best fit to the PSC composite data for these particles was given by the model proposed by Fricke in which the Maxwell−Wagner dispersion is extended to a suspension of ellipsoids (platelike).[60] The crossover point between the fitted data and the simple electrolytic NaCl solution gives the bulk conductivity. The measured conductivity at room temperature for the as-synthesized BiCuOS samples is 0.08(2) S cm^{-1} (Figure 8). Although modest, the conductivity of hydrothermally prepared BiCuOS is significantly greater than values reported previously for powder samples of LnCuOS (Ln = La, Pr, and Nd). For example, the reported conductivity for a cold-pressed, then sintered pellet of LaCuOS was 8.0×10^{-6} S cm^{-1}, and the conductivities of nondoped PrCuOS (1.6×10^{-5} S cm^{-1}) and NdCuOS (3.8×10^{-4} S cm^{-1}) were also lower than that of the present BiCuOS.[11] This is somewhat surprising because, as shown in Figure 7, the orbital contribution to the valence bands of both LaCuOS and BiCuOS are qualitatively similar and result from the considerable overlap between copper 3*d* and sulfur 3*p* states in the $(Cu_2S_2)^{2-}$ layers, reflecting the strong covalent character of the Cu−S bonds. As a result of this large dispersion near the VBM and because photoluminescence measurements (Ln = La, Pr, and Nd) indicate that excitons are confined in the $(Cu_2S_2)^{2-}$ layer,[11] both LaCuOS and BiCuOS should exhibit similar electrical conductivities. Instead, the conductivity of BiCuOS compares well to that of CeCuOS (0.61 S cm^{-1}) and CeAgOS (0.16 S cm^{-1}).[8,11] Indeed, BiCuOS, CeCuOS, and CeAgOS are all black and exhibit conductivities similar to that of strontium-doped LnCuOS (Ln = La, Pr, and Nd) powder samples. The higher conductivity of the cerium oxysulfides has been ascribed to ionic (CeAgOS) and semimetallic (CeCuOS) conduction mechanisms. Because CeAgOS is isostructural to LaAgOS, a known ionic conductor,[61,62] and similar in chemical composition to other ionic conductors (Ag_2S, Ag_2Se, and $Ag_4Hf_3S_8$), Chan and coworkers have proposed that CeAgOS is very likely an ionic conductor.[8] Ueda et al. have proposed on the basis of ultraviolet and inverse photoemission spectroscopic measurements that the increased electrical conductivity of CeCuOS results from the presence an empty conduction band near the Fermi level, placing CeCuOS in a semimetallic state.[11] Owing to the absence of silver in BiCuOS and the presence of the unoccupied conduction band near the Fermi level composed of bismuth 6*p* orbitals, the optical and electrical

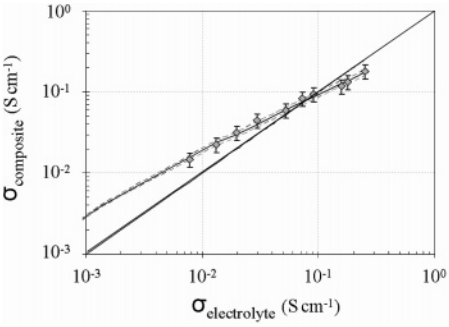

Figure 8. Graph that summarizes the powder-solution-composite conductivity measurements for BiCuOS. A conductivity estimate is given where the composite (gray diamonds) and electrolyte conductivities are equivalent. A model proposed by Fricke (best-fit line), in which the Maxwell−Wagner dispersion was extended to a suspension of ellipsoids (platelike), was used to fit the data.[60]

(53) Seshadri, R. *Solid State Sci.* **2006**, *8* (3−4), 259−266.
(54) Payne, D. J.; Egdell, R. G.; Walsh, A.; Watson, G. W.; Guo, J.; Glans, P. A.; Learmonth, T.; Smith, K. E. *Phys. Rev. Lett.* **2006**, *96* (15), 157403/1−157403/4.
(55) Meredith, R. E.; Tobias, C. W. *Adv. Electrochem. Electrochem. Eng.* **1962**, *2*, 15−47.
(56) Douglas, J. F.; Garboczi, E. J. *Adv. Chem. Phys.* **1995**, *91*, 85−153.
(57) Garboczi, E. J.; Douglas, J. F. *Phys. Rev. E: Stat. Phys., Plasmas., Fluids., Relat. Interdiscip. Top.* **1996**, *53*, 6169−6180.
(58) McLachlan, D. S.; Hwang, J. H.; Mason, T. O. *J. Electroceram.* **2000**, *5* (1), 37−51.
(59) Campo, M. A.; Woo, L. Y.; Mason, T. O.; Garboczi, E. J. *J. Electroceram.* **2002**, *9* (1), 49−56.
(60) Fricke, H. *J. Phys. Chem.* **1953**, *57*, 934−7.
(61) Wilmer, D.; Jorgensen, J. D.; Wuensch, B. J. *Solid State Ionics* **2000**, *136*, 961−966.
(62) Palazzi, M.; Carcaly, C.; Flahaut, J. *J. Solid State Chem.* **1980**, *35* (2), 150−155.

transport properties of BiCuOS more closely resemble those of semimetallic CeCuOS.

Conclusions

BiCuOS can be efficiently prepared via a hydrothermal reaction between Bi_2O_3, Cu_2O, and Na_2S at a considerably lower reaction temperature (250 °C) and time (48 h) than in previously reported solid-state reactions. Solubility data for the bismuth and rare-earth sesquioxides provide insight into why BiCuOS forms in a hydrothermal reaction whereas LnCuOS phases do not. The measured conductivity of hydrothermally prepared BiCuOS is similar to that of CeCuOS and CeAgOS, and is markedly greater than the values reported previously for nondoped polycrystalline LnCuOS materials (Ln = La, Pr, and Nd). However, owing to scalar relativistic effects that significantly lower the energy of the conduction band, BiCuOS is black, which precludes its use as a transparent conductor. Indeed, the optical, electrical transport properties, and band structure of BiCuOS are similar to those of semimetallic CeCuOS. In general, these results highlight why the presence of a more electropositive rare-earth ion (e.g., La^{3+}) in the structure is necessary to shift the conduction band toward higher energy and thus increase the optical band gap.

Acknowledgment. The authors thank R. Seshadri who contributed the theoretical calculations. We gratefully acknowledge support from the Department of Energy, National Renewable Energy Laboratory Subcontract (Award No. XAT-5-33636-02/DE-AC36-98GO). The authors made use of Central Facilities supported by the MRSEC program of the National Science Foundation (Grant DMR-0520513) at the Materials Research Center of Northwestern University. The SEM and EDX were performed by Matt Russell and Warefta Hasan, respectively, in the EPIC facility of the NUANCE Center at Northwestern University. NUANCE Center is supported by NSF-NSEC, NSF-MRSEC, Keck Foundation, the State of Illinois, and Northwestern University. W.C.S was additionally supported through a Natural Science and Engineering Research Council of Canada (NSERC) Julie Payette post-graduate doctoral scholarship.

Supporting Information Available: Energy dispersive X-ray (EDX) spectroscopy data. This material is available free of charge via the Internet at http://pubs.acs.org.

IC7014622